Breast Cancer Research

RESEARCH

Open Access

Serum metabolomic profiling for predicting therapeutic response and toxicity in breast cancer neoadjuvant chemotherapy: a retrospective longitudinal study

Zhihao Fang[1,2†], Guohong Ren[1,2†], Shouyu Ke[1,2†], Qimin Xu[1,2], Yuhua Chen[5], Xiaoyuan Shi[6], Cheng Guo[3,4*] and Jian Huang[1,2,3,4*]

Abstract

Background Neoadjuvant chemotherapy (NACT) is the standard-of-care treatment for patients with locally advanced breast cancer (LABC), providing crucial benefits in tumor downstaging. Clinical parameters, such as molecular subtypes, influence the therapeutic impact of NACT. Moreover, severe adverse events delay the treatment process and reduce the effectiveness of therapy. Although metabolic changes during cancer treatment are crucial determinant factors in therapeutic responses and toxicities, related clinical research remains limited.

Methods One hundred paired blood samples were collected from 50 patients with LABC before and after a complete NACT treatment cycle. Untargeted metabolomics was used by liquid chromatography-mass spectrometry (LC–MS) to investigate the relationship between dynamically changing metabolites in serum and the responses and toxicities of NACT.

Results Firstly, we observed significant alterations in serum metabolite levels pre- and post-NACT, with a predominant enrichment in the sphingolipid and amino acid metabolism pathways. Second, pre-treatment serum metabolites successfully predicted the therapeutic response and hematotoxicities during NACT. In particular, molecular subtype variations in favorable treatment responses are linked to acyl carnitine levels. Finally, we discovered that the therapeutic effects of NACT could be attributed to essential amino acid metabolism.

Conclusion This study elucidated the dynamic changes in metabolism during NACT treatment, providing a possibility for developing responsive metabolic signatures for personalized NACT treatment.

Keywords Breast cancer, Neoadjuvant chemotherapy, Serum, Metabolomics, Acylcarnitine, Essential amino acid

†Zhihao Fang, Guohong Ren and Shouyu Ke these authors contributed equally.

*Correspondence:
Cheng Guo
cheng_guo@zju.edu.cn
Jian Huang
drhuangjian@zju.edu.cn
Full list of author information is available at the end of the article

Introduction

Breast cancer is the most commonly diagnosed cancer and the leading cause of cancer-related death among women worldwide, with its incidence expected to increase significantly over the next two decades [1]. Owing to geographic and socioeconomic variations, approximately 5%–40% of patients are diagnosed with locally advanced breast cancer (LABC) at the first visit, which has a worse prognosis than early breast cancer due to a higher likelihood of local recurrence and distant metastasis after surgery [2–4]. Furthermore, LABC is defined here as breast cancer confined to the breast and local lymph nodes without distant metastasis, including stages IIB and IIIA–C. Neoadjuvant chemotherapy (NACT) is crucial in the initial treatment of LABC as it reduces tumor burden and increases the rate of breast-conserving surgery [5]. Consequently, NACT plus surgery was considered the standard treatment for LABC. However, patients showed significant variability in response to NACT, highlighting the urgent need for personalized treatment strategies. Clinical statistics showed that only 20%–30% of patients with LABC can achieve pCR [6, 7]. In clinical practice, preoperative examinations, including needle biopsy, immunohistochemistry, ultrasound, mammography, and magnetic resonance imaging, have been employed to formulate NACT plans and assess efficacy [8]. However, these techniques fail to provide reliable assessments, impeding the provision of individualized NACT therapy for patients with LABC.

The treatment response of patients with LABC to NACT depends on many genetic and clinical factors. During NACT treatment, patients with LABC may experience various adverse effects, including anemia, leukopenia, and thrombocytopenia [9, 10]. Chemotherapy-induced hematotoxicity leads to cessation of treatment in patients who cannot tolerate it. Hence, identifying early predictive markers for NACT treatment is imperative, especially those capable of predicting drug response and toxicities before treatment, to screen sensitive populations and minimize adverse effects, thereby enhancing patient benefits.

Molecular subtypes of breast cancer are crucial to the efficacy of NACT. The pCR rate varied among subtypes, with the hormone receptor (HR)-positive human epidermal growth factor receptor 2 (HER2)-negative subtype (luminal type) showing significantly lower rates than the HER2-positive and triple-negative subtypes (collectively known as non-luminal type) [6, 7]. However, it remains unclear why a subtype-specific difference exists. Furthermore, variations in pCR rates among patients with HER2-positive LABC may be caused by variables such as the degree of HER2 amplification and whether the regimen included pertuzumab [11, 12]. Therefore, the clinical results of NACT treatment for patients with LABC are influenced by many important factors.

Metabolomics encompasses the comprehensive measurement of metabolites within biological systems, offering a molecular understanding of pathogenic characteristics [13, 14]. It is widely acknowledged that metabolic instability is vital in the development of breast cancer, including aberrant glycolysis, choline metabolism, glutamine metabolism, lipid biosynthesis, tricarboxylic acid cycle, pentose phosphate pathway, and fatty acid metabolism [15–17]. Nonetheless, studies on the reactive metabolic traits of NACT are limited. Although several studies have reported metabolic changes in patients with breast cancer undergoing chemotherapy [18–20], clinical cohort studies on the metabolomics of patients with LABC receiving NACT treatment are rather limited [21, 22].

Therefore, this study conducted an untargeted metabolomic analysis of a clinical cohort of patients with LABC to determine the metabolic characteristics of NACT in patients with breast cancer. Here, we examined 100 serum samples from 50 patients with LABC to identify sensitive metabolic characteristics connected to NACT treatment both before and after. In our small-scale clinical cohort, the distribution of breast cancer subtypes was as follows: 19 patients had luminal type, 20 patients were HER2-positive, and 11 patients were triple-negative. A total of 12 patients achieved pCR after NACT treatment. Pathological tests of postoperative specimens in patients with NACT were performed to determine the Miller and Payne (MP) grade [23]. Based on the prognostic potential of the MP grading system, we defined a responsive (R) group (MP grades 4–5) and a non-responsive (NR) group (MP grades 1–3) [24, 25]. We further investigated the connection between serum metabolic profiles and favorable therapeutic responses. In particular, we discovered a correlation between the molecular subtype difference in R to NACT and the levels of acylcarnitines. Finally, we compared the metabolic changes and clinical outcomes before and after complete treatment with NACT, revealing significant differences in essential amino acid metabolism between the R and NR patients. In conclusion, our research findings have unveiled the metabolic dynamics of NACT treatment, offering enormous potential for guiding personalized NACT therapy based on serum metabolic features.

Methods

Sample collection

This study protocol has been approved by the Ethics Committee of the Second Affiliated Hospital of Zhejiang University (SAHZU), Hangzhou, China. From September 2022 to December 2023, serum samples (n = 100) from 50 patients with LABC were collected from the Clinical Laboratory of SAHZU. Eligible patients were all females aged between 35 and 75 years old, diagnosed with clinical T2-4 and N^+ breast cancer, including IIB, and IIIA-C stage. The inclusion criteria included pathology of tumor and lymph node suggested invasive ductal carcinoma; imaging report indicated the maximum diameter of the tumor ≥ 2 cm; performed the complete course of chemotherapy. The exclusion criteria included as follows: (1) history of other malignant tumors; (2) special types of breast cancer (e.g., papillary carcinoma, squamous cell carcinoma); (3) severe liver and kidney diseases leading to abnormal liver and kidney function (aspartate aminotransferase, alanine aminotransferase, and alkaline phosphatase levels > 3 times the upper limit of normal; creatinine concentration exceed the upper limit of normal). All enrolled patients have signed informed consent forms. All patients received 4 cycles of epirubicin combined with cyclophosphamide treatment followed by 4 cycles of paclitaxel treatment or 6 cycles of paclitaxel combined with platinum drug treatment. All HER2-positive patients received dual-targeted therapy with trastuzumab combined with pertuzumab. In this study, according to postoperative pathological results, an MP grade of 5 was considered as pCR, while grades of 4–5 were considered as the response (R) to NACT treatment. Serum samples for each patient were collected at two-time points: before the first chemotherapy and before surgery. For serum collection, all participants were required to fast overnight and collect 5 mL of peripheral venous blood in the morning.

Reagents and sample preparation

Water (H_2O) was obtained from a Milli-Q water purification apparatus (Millipore, Milford, MA, USA). Liquid chromatography-mass spectrometry (LC − MS) grade methanol (MeOH) and acetonitrile (ACN) were bought from Merck KGaA (Darmstadt, Germany) and chromatographic grade formic acid (FA) was obtained from Fluka (Muskegon, MI, USA). Three isotopically labeled chemical standards of metabolites were purchased from MedChemExpress (Shanghai, China). Serum samples (50 μL) were extracted using a 200 μL mixture of methanol:acetonitrile (2:1) containing internal standards (d3-leucine, d3-palmitoyl carnitine, and d4-cholic acid). The samples were incubated at − 20 ℃ for 1 h after vortexing for 30 s and sonicated for 1 min. Then, the samples were centrifuged at 14,000 rpm for 15 min at 4℃ to remove protein precipitate. Next, vacuum-dried 100 μL of supernatant was stored at − 80 ℃. Prior to LC–MS analysis, drained samples were dissolved with 100 μL of 20% acetonitrile water, centrifuged at 14,000 rpm for 15 min, and then took the supernatant into HPLC vials.

LC − MS analysis

Analyses were performed using an Acquity UPLC system (Waters, USA) connected to a TripleTOF 6600 mass spectrometer (AB SCIEX, USA). A UPLC HSS T3 column (1.8 μm; 100 mm in length × 2.1 mm in diameter) was used for separation with the column temperature maintained at 25 °C. Mobile phase A was water with 0.1% FA, and B was ACN with 0.1% FA. The flow rate was 0.35 mL/min and the gradient was set as follows: 0–1 min: 1% B;1–18 min: 1% B to 50% B; 18–18.5 min: 50% B to 100% B; 18.5–22.5 min: 100% B; 22.5–23 min: 100% B to 1% B; 23–26 min: 1% B. The injection volume was 5 μL. Random analysis was performed on all samples during the data collection process. The quality control (QC) sample was prepared by combining aliquots of all subject samples. The QC sample was injected every 10 samples.

The ESI source conditions on TripleTOF were as follows: Gas Source 1 (GS1) was set at 60 psi, Gas Source 2 (GS2) was set at 60 psi, Curtain Gas (CUR) was set at 30 psi, Source Temperature was 600 °C, and IonSpray Voltage Floating (ISVF) was set at 5500 V in positive ion mode. The instrument was configured to scan and collect the *m/z* range of 60–1000 Da through TOF MS, and the *m/z* range of 25–1000 Da for product ion scanning. The accumulation time for TOF mass spectrometry scans was set at 0.20 s/spectra, while the product ion scan was set at 0.05 s/spectra. Acquired product ion scan was used Information Dependent Acquisition (IDA) with high sensitivity mode. In the full scan experiment, IDA triggers MS/MS based on a set of user-input standards. The unit resolution for selecting precursor ions, with collision energy (CE) fixed at 35 ± 15 eV. The declustering potential (DP) was set as 60 V [26].

Metabolomics data processing

The metabolomics data processing method follows the protocols outlined in a previous publication [27, 28]. The original MS data (wiff.scan) files were converted to mzXML format using ProteoWizard MSConvert (version 3.0) [29], and MA-DIAL (version 4.9) [30] was utilized for peak detection, retention time correction, and peak alignment. The parameters set for MS-DIAL processing are as follows: peak detection quality accuracy = 10 ppm; peak width c = (5,30); snthresh = 3; minfrac = 0.5. For each metabolic feature, intensities of more

than 5 standard deviations were considered outliers and set as missing values. Data with missing values exceeding 70% will be removed. The remaining missing values are calculated and filled using the k-Nearest Neighbors (KNN) algorithm [31]. Metabolite peaks with relative standard deviations (RSDs) less than 30% in QC samples were used for subsequent analysis.

Metabolite identification was performed using the previously published software MetDNA2 (http://metdna.zhulab.cn/)(28). In brief, this tool utilized an internal metabolite spectral library to annotate metabolites by matching accurate mass, retention time, and MS/MS similarity and categorized them into metabolomics standards initiative (MSI) level 1 and MSI level 2 based on the degree of matching. Metabolites identified by matching with external public metabolite libraries and lipid spectral libraries were considered as MSI level 3 [32]. The MS/MS similarity was calculated using the dot product algorithm, with the cut-off point set at 0.8. All metabolite and lipid identification values can be found in Additional file 1. Three internal standards were added to each sample to monitor the reproducibility of the LC–MS data acquisition process, with RSDs of peak areas being 7.7%, 7.2% and 4.0%, respectively (Additional file 6: Fig. S1a). After data normalization, the median RSDs of metabolites determined by reversed-phase liquid chromatography-mass spectrometry (RPLC-MS) were 12.5% (Additional file 6: Fig. S1b). The reproducibility of QC samples was evaluated using principal component analysis (PCA), and the results showed that QC samples clustered closely together in the PCA plot (Additional file 6: Fig. S1c). The above results indicated that this method has good data quality and excellent reproducibility.

Statistical analyses

The statistical analyses were performed using IBM SPSS Statistics (version 24.0) and R (version 4.3.2) [33]. Multivariate analyses were performed by R package "mixOmics" (version 6.26.0), including supervised partial least squares discriminant analysis (PLS-DA), from which variable projected importance (VIP) values for each metabolite were obtained. The univariate analysis assessed the statistical significance (P value) and fold change (FC) between two groups for each metabolite based on the two-sided Wilcoxon test. The criteria for identifying differentially expressed metabolites were P value < 0.05, FC > 1.5 or < 0.66 and VIP > 1. The volcano plot was created using the R package "ggplot2". Pathway enrichment analysis utilized MetaboAnalyst (https://www.metaboanalyst.ca/)(34), embedded with the Kyoto Encyclopedia of Genes and Genomes (KEGG) pathway database [35]. After normalizing the data by z-scores, hierarchical clustering analysis was generated using the R package "pheatmap".

Using the R package "glmnet" (version 4.0.2) for feature selection via adaptive lasso [36]. At first, all metabolites and clinical covariates (age, BMI, Ki-67, and stage) were graded and used for the selection of predictors. The adaptive weight vector ω was calculated using the initial estimates of the coefficients obtained from the main tenfold cross-validation, used as a penalty factor in the lasso regression subsequently. The optimal lambda was chosen by a tenfold cross-validation. After feature selection, a binary logistic regression model was constructed using SPSS to predict the probability of R to NACT using baseline serum metabolites. Additionally, considering the relatively small sample size, we limited the number of predictive factors in the final model to four. The logical model for predicting the chances of R using four predictor factors culminated in a formula. Randomly selected 60% of the patients from the dataset as the training data to establish a predictive model, with the remaining 40% of patients as the validation data. The random sampling was repeated 1000 times to build and validate the model. Similarly, SPSS was used to plot receiver operating characteristic (ROC) curves and calculate the area under the curve (AUC) value and 95% confidence interval (CI).

The two-way ANOVA analysis was conducted using the R function "aov". Metabolites with $P < 0.05$ of NACT, R, and interaction dimensions were selected separately. Used non-parametric Wilcoxon rank-sum test to compare the differences in metabolite levels between R and NR patients. To calculate the correlation between amino acids, the R package "Hmisc" was used for Pearson correlation.

Results

Serum metabolic traits in response to NACT in patients with LABC

This study recruited 50 patients diagnosed with clinical T2-4 and N + breast cancer from the Second Affiliated Hospital Zhejiang University School of Medicine, Hangzhou, China. All enrolled patients received conventional NACT regimens, followed by complete breast resection or preservation surgery. Additional file 6: Table S1 includes detailed information about the clinical cohort. To study NACT's impact on serum metabolic profiles, we collected two blood samples from each patient with breast cancer before the first chemotherapy and surgery (Fig. 1a).

Serum samples from 50 patients with LABC underwent untargeted metabolomics analysis using RPLC-MS. In total, 265 metabolites were identified based on the metabolomics standards initiative [32] (Fig. 1b and Additional file 1). Unsupervised principal component analysis

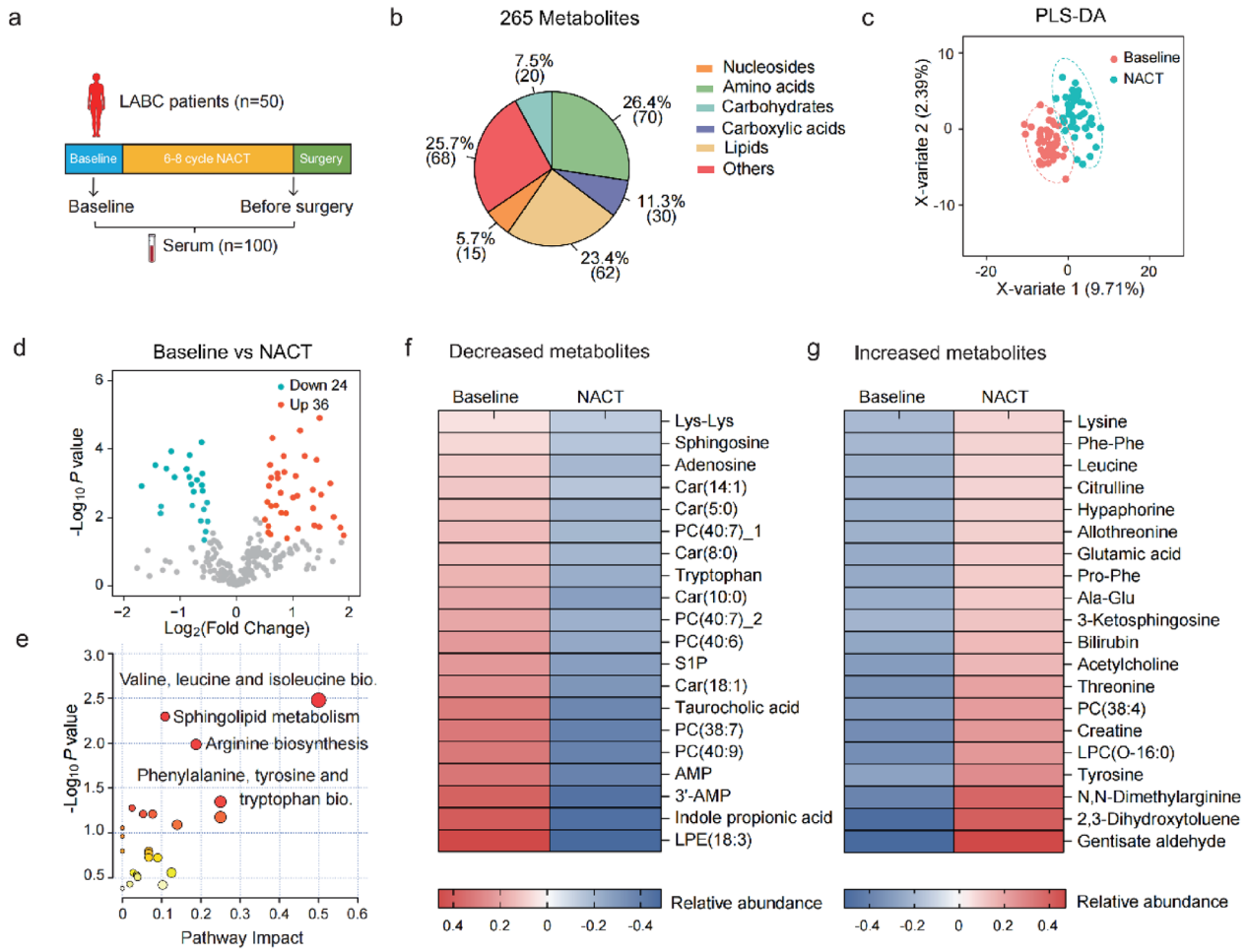

Fig. 1 Serum metabolic characteristics of LABC patients in response to NACT. **a** Clinical design overview of metabolomics study. **b** Number of identified metabolites in the serum sample and the distribution of their chemical categories. **c** Principal component analysis (PCA) reveals significant changes in metabolic profiles before and after NACT treatment. **d** Volcano plot of metabolites significantly associated with NACT treatment (P value < 0.05, FC > 1.5 or < 0.66). Aquamarine dots (n = 24) and orange dots (n = 36) represent metabolites that were increased and decreased, respectively, before and after NACT treatment. The grey dots represent unchanged metabolites. **e** Pathway enrichment analysis of metabolites (n = 60) significantly altered before and after NCAT (Hypergeometric test; P < 0.05). The pathway enrichment was performed using MetaboAnalyst. **f, g** Heatmaps show the top 20 decreased (f) and top 20 increased (g) metabolites associated with NACT treatment

revealed significant differences in the metabolic profiles of serum samples between two-time points, indicating metabolic changes following the completion of NACT (Fig. 1c). Furthermore, we used univariate and multivariate analyses to identify metabolites associated with NACT treatment, revealing 60 metabolites exhibiting significant changes ($P < 0.05$, FC > 1.5 or < 0.66, VIP > 1; Additional file 2). Among these, the volcano plot revealed that 36 metabolites increased and 24 metabolites decreased following NACT treatment (Fig. 1d). The metabolic pathway enrichment analysis results demonstrated that the changed metabolites were enriched in sphingolipid metabolism and amino acid metabolism, such as phenylalanine, tyrosine, and tryptophan biosynthesis; arginine biosynthesis; and valine, leucine, and isoleucine biosynthesis (Fig. 1e). Through further analysis, we listed the top 20 differential metabolites that increased and decreased after NACT treatment (Figs. 1f–g). Overall, comprehensive metabolomics has demonstrated that NACT treatment induces significant changes in the metabolic profile of patients with LABC during the NACT treatment process.

Metabolic traits before treatment predict NACT-induced hematologic toxicity

Patients undergoing NACT frequently suffer from hematological toxicity, which can lead to treatment interruption in patients unable to tolerate it and reduce the

therapeutic efficacy of NACT. Subsequently, we investigated the correlation between metabolite levels before treatment and usual hematological toxicities, encompassing the nadir levels of hemoglobin (Hb), white blood cells (WBC), platelets (PLT), and neutrophils (NEUT) during treatment. We found that 53 metabolites in different categories were significantly associated with at least one hematological toxicity ($P < 0.05$; Fig. 2a and Additional file 3). Pathway enrichment analysis revealed significant enrichment of metabolites associated with WBC and NEUT in similar metabolic pathways, such as phenylalanine, tyrosine, and tryptophan biosynthesis; as well as D-amino acid metabolism (Fig. 2b). Furthermore, the metabolites associated with Hb and PLT were significantly enriched in the pyrimidine metabolic pathway (Fig. 2b). We exhibited examples of the correlation

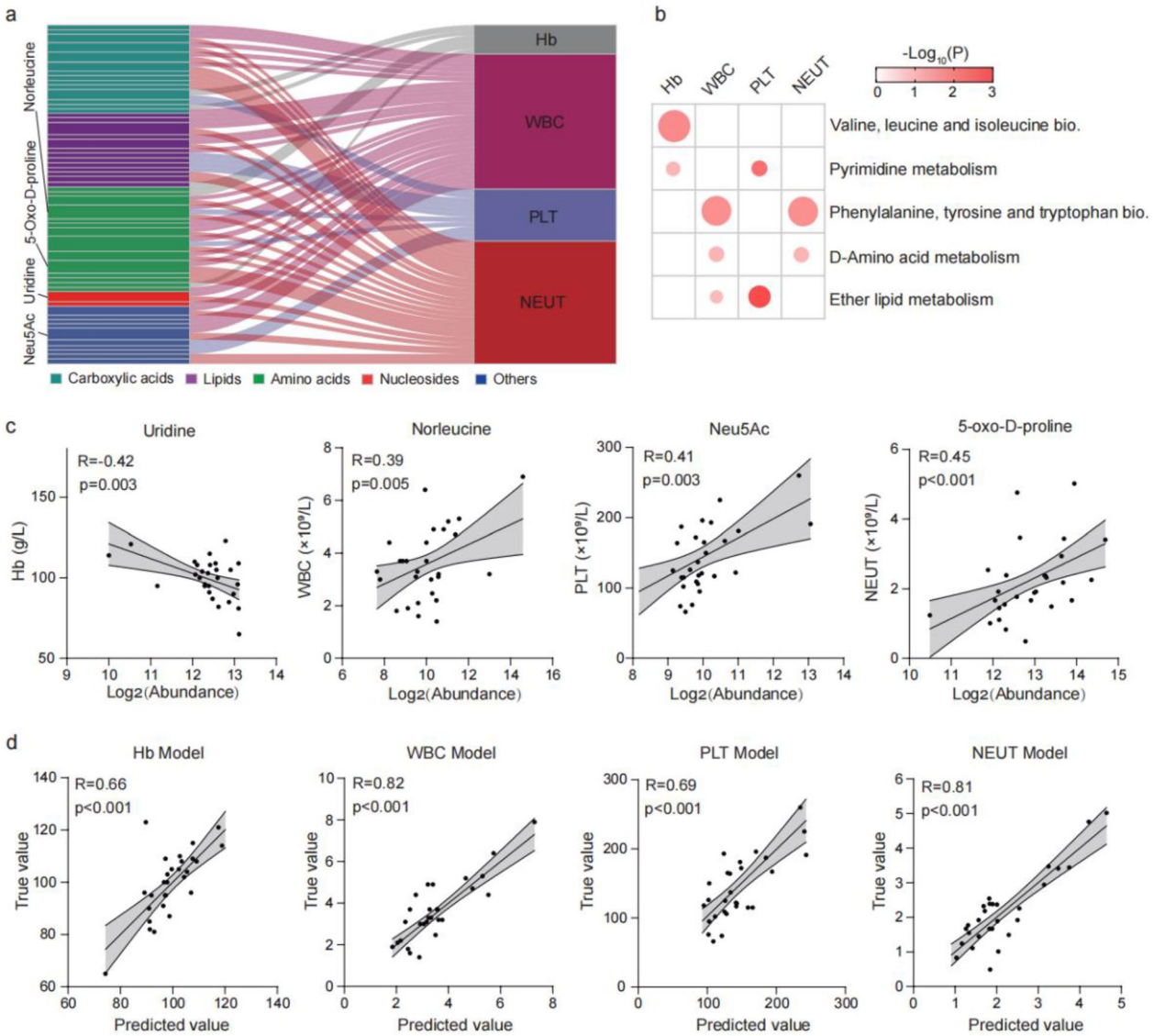

Fig. 2 Pre-therapeutic metabolic traits predict the hematologic toxicities caused by NACT. **a** Significant correlation between the lowest counts of the four cell types associated with hematological toxicity and the pre-treatment serum metabolites. (Pearson correlation; two-sided Student's t test $P < 0.05$). Hb, hemoglobin; WBC, white blood cells; PLT, platelets; NEUT, neutrophils. **b** Pathway enrichment analyses of hematologic toxicity associated metabolites (Hypergeometric test; $P < 0.05$). **c** Four examples of metabolites and their relevance to hematological toxicity. (Pearson correlation; two-sided Student's t test $P < 0.05$). Neu5Ac, N-Acetylneuraminic acid. Error bands represent 95% confidence intervals. **d** Multiple linear regression models constructed from different serum baseline metabolites to predict nadir cell counts and hematological toxicity during NACT. (Pearson correlation; two-sided Student's t test $P < 0.05$). Error bands represent 95% confidence intervals. Supplementary Tables 3–6 provide details of the prediction models

between specific metabolites and each hematological toxicity in Fig. 2c, including uridine, norleucine, N-acetylneuraminic acid, and 5-oxo-D-proline. To further validate the relationship between pre-treatment metabolites and hematological toxicity, we predicted each type of hematotoxicity using its respective correlated metabolites. We applied all relevant metabolites to a multiple linear regression (MLR) model to construct Hb predictive models. We first selected key metabolites using lasso regression for WBC, PLT, and NEUT and then constructed MLR models. Consequently, we selected 6, 13, 7, and 13 metabolites to predict Hb, WBC, PLT, and NEUT values, respectively (Fig. 2d and Additional file 6: Tables S2–S5). Each generated predictive model demonstrated a significant positive correlation between its predicted values and the clinically measured results (Fig. 2d). In conclusion, we suggest that pre-treatment metabolic traits can successfully predict the occurrence of hematological toxicity adverse events during NACT treatment, further demonstrating the pivotal role of serum metabolic profiles in NACT-induced toxicities.

Key metabolites predict the therapeutic response of NACT

After completing NACT treatment, about 20% to 30% of patients achieved pCR and demonstrated better prognoses than those who did not achieve pCR [6, 7]. Therefore, early prediction of the response to NACT treatment is crucial. To investigate the metabolic profile associated with drug response, we analyzed metabolomics data from baseline levels in R (n = 18) and NR (n = 32) patients before initiating NACT. There were 15 metabolites linked to improved therapeutic response in the initial analysis ($P < 0.05$; Fig. 3a). Pathway analysis showed significant enrichment of these metabolites in phenylalanine, tyrosine, and tryptophan biosynthesis; phenylalanine metabolism; nicotinate and nicotinamide metabolism; and valine, leucine, and isoleucine biosynthesis (Fig. 3b). After that, we created a logistic regression model to predict the chances of R in patients with LABC before receiving NACT after using lasso regression to select key metabolites (Fig. 3c). For the prediction model, the clinical covariate of breast cancer subtype and three metabolites, such as leucine, phosphatidylcholine (PC) (36:3), and hypoxanthine, were ultimately selected (Fig. 3d and Additional file 6: Table S6). With a diagnostic specificity of 91% and sensitivity of 72%, the expected cutoff value is 0.50 (Fig. 3e). Good discriminant performance was also confirmed by the receiver operating characteristic curve (area under the curve = 0.91; 95% confidence interval: 0.84–0.99; Fig. 3f). Notably, this model could be used to predict all MP grades after NACT in patients with LABC (Additional file 6: Fig. S2a). These results indicated significant differences in pre-treatment metabolic characteristics among patients with LABC who have received NACT treatment, and the pre-treatment metabolic traits might identify individuals who are sensitive to NACT treatment, helping predict a favorable therapeutic response.

Acyl carnitines are associated with a better therapeutic response in patients with non-luminal breast cancer

Previous studies have reported that the difference in pCR rates after NACT was related to the breast cancer subtype, with HR-positive HER2-negative, also known as luminal, being a risk factor [6]. In our study, the treatment response rate was significantly lower in patients with the luminal subtype than in those with the non-luminal subtype ($P = 0.08$; Chi-square test; Fig. 4a). We then investigated the disparities in metabolic characteristics at baseline associated with treatment response induced by NACT among breast cancer subtypes.

The comparative analysis of metabolites in patients with luminal and non-luminal subtypes responding to treatment showed that 21 metabolites were related to subtype and therapeutic response ($P < 0.05$). Among these, 10 metabolites showed no difference across all subtypes when the treatment response was not stratified (Fig. 4b), suggesting that these metabolites are subtype-specific only to R patients. Further examination revealed significant associations between four carnitines (Cars (3:0), (8:1), (10:3), and (18:0)) and subtype-specific differences in the R patients. Interestingly, the total serum carnitine levels of 20 carnitines detected in R patients with luminal subtypes were significantly higher than those in patients with non-luminal subtypes (Fig. 4c and Additional file 4). As a comparison, no subtype differences in total carnitine levels were observed in any patients. For instance, the levels of Car (18:0) were higher in R patients with the luminal subtype than in R patients with the non-luminal subtype, while no difference was observed in all patients with comorbidities (Fig. 3d). Similar results regarding Cars (3:0), (8:1), and (10:3) can be found in Additional file 6: Fig. S2b. Additional file 6: Fig. S3 shows a comparison of the individual and total carnitine levels among the four groups (luminal type R, luminal type NR, non-luminal type R, and non-luminal type NR). In addition, subsequent analyses of carnitine based on unsaturation and carbon number showed more subtype-specific variations. Saturated short- and medium-chain carnitine ($C < 5$ and $5 \leq C \leq 12$) did not reveal any subtype differences, whereas saturated long-chain carnitine ($C > 12$) in R patients showed substantial differences between luminal and non-luminal types (Fig. 3e). Furthermore, medium-chain unsaturated carnitine with one and three carbon–carbon bonds held subtype differences in R patients before NACT. Overall, these findings

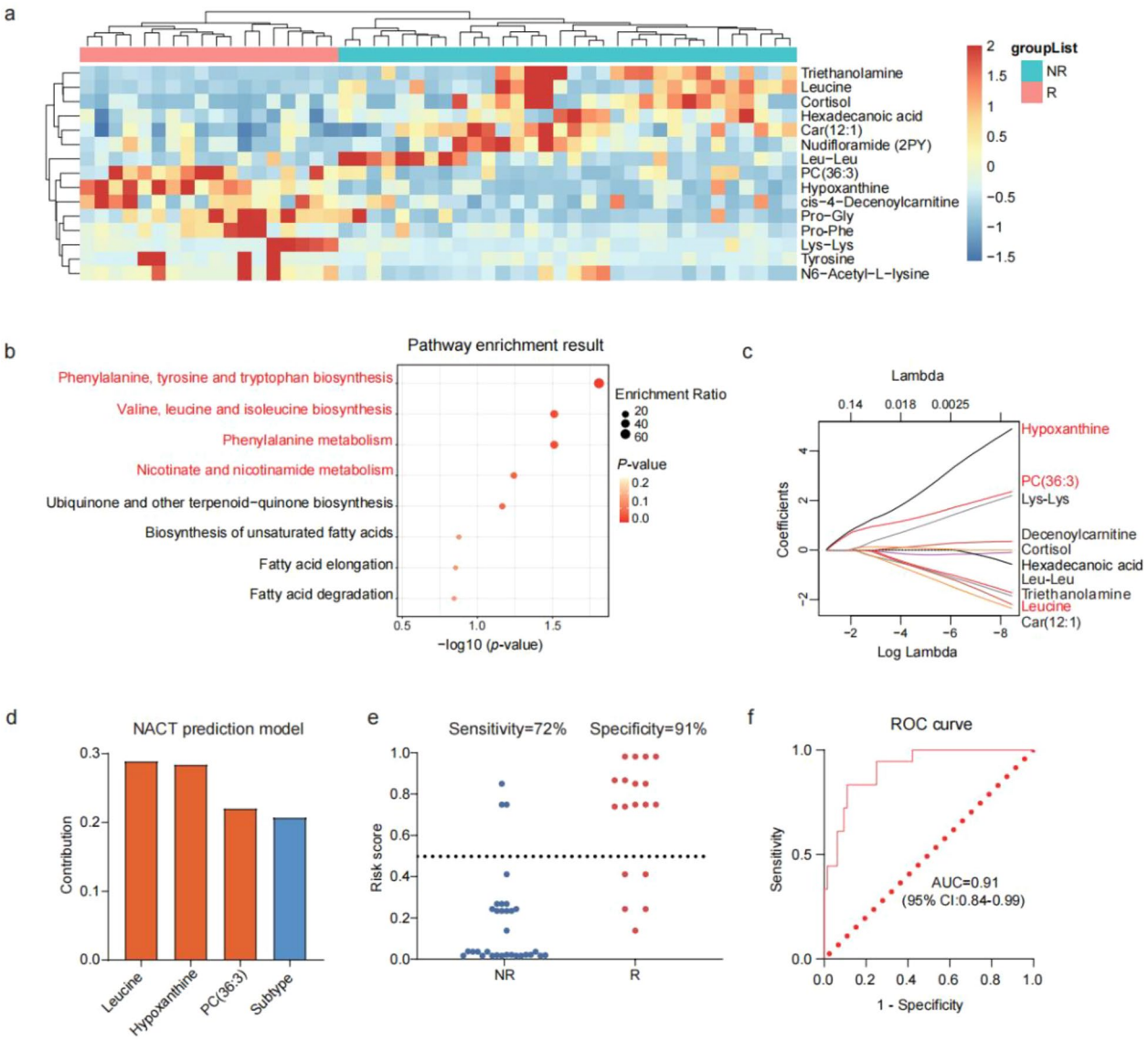

Fig. 3 Predictive model for therapeutic efficacy based on key serum metabolites. **a** Heatmap revealed baseline metabolites significantly correlated with response (R) to NACT ($P < 0.05$; Two-sided Student T test). **b** Pathway enrichment analysis ($P < 0.05$; Hypergeometric test). **c** Lasso regression for the selection of key metabolites. **d** Selected key metabolites and breast cancer subtype for the logistic regression model to predict the chances of R. **e** The sensitivity and specificity of the prediction model with a risk score of 0.5 (R: n = 18; NR: n = 32). **f** Receiver operating characteristic curve of the logistic regression model

unequivocally suggest that variations in metabolism among subtypes are linked to post-NACT therapeutic response.

Increased essential amino acids are beneficial to R in NACT

Using a two-way ANOVA analysis, 60 and 15 metabolites were identified to be associated with NACT and R status, respectively. In addition, we found that 24 metabolites exhibited significant interactions with NACT and R states (within the red circles; Fig. 5a). Pathway enrichment analysis of these metabolites revealed a notable enrichment of pathways related to amino acids (Fig. 5b). Next, we examined how amino acids coordinate their metabolism in R and NR patients before and after NACT treatment. According to Pearson's correlation analysis, seven positively associated amino acids, five of which were essential, were found in R patients. Nevertheless, among the NR patients, there was only one positive correlation (Fig. 5c, Additional files 5, 6). Before NACT treatment, further examination of total, essential,

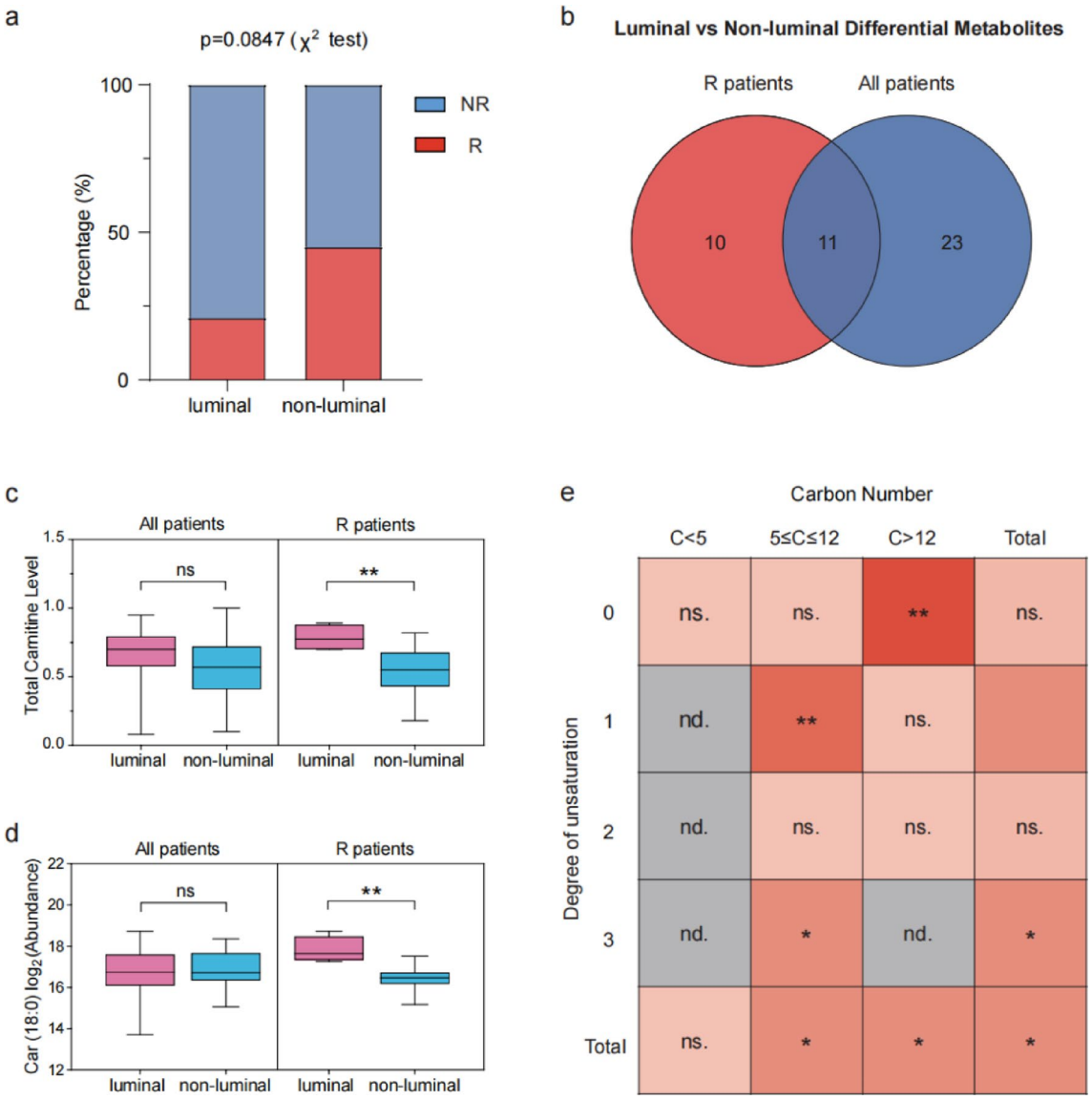

Fig. 4 Acyl carnitines are associated with subtype differences in R status following NACT. **a** Non-Luminal patients had a significantly higher chance of achieving R than Luminal ($P = 0.08$; χ^2 test). **b** Venn plot showed the number of metabolites associated with the subtype in R patients (red) and all patients (blue). **c, d** All patients (Luminal = 19, non-Luminal = 31) and R patients (Luminal = 4, non-Luminal = 14) total carnitine and Car (18:0) levels. **e** Subtype disparity in carnitine levels associated with R status after NACT. (nd, not detected; **, $P < 0.01$; *, $P < 0.05$; ns, not significant; Two-sided Wilcoxon test)

and non-essential amino acids revealed no distinctions between R and NR patients at baseline. (Fig. 5d). Notably, R patients demonstrated significantly higher levels of total and essential amino acids after completing NACT than NR patients. However, no variations were observed in the levels of non-essential amino acids (Fig. 5e). Comparing individual amino acid revealed higher levels of most essential amino acids (isoleucine, valine, methionine, phenylalanine, and threonine) in R patients than in NR patients. However, for non-essential amino acids, no significant difference was observed between the two groups (Fig. 5f). In addition, the odds ratio for each amino acid was determined using a logistic regression model, and their contributions to the R status were examined (Fig. 5g). The results demonstrated that the odd ratios of glutamine, isoleucine, lysine, methionine, tryptophan, threonine, and valine are higher than 1, suggesting that R in NACT benefits from increased levels of these amino acids. In conclusion, amino acids are critical metabolic features that reflect the response of patients

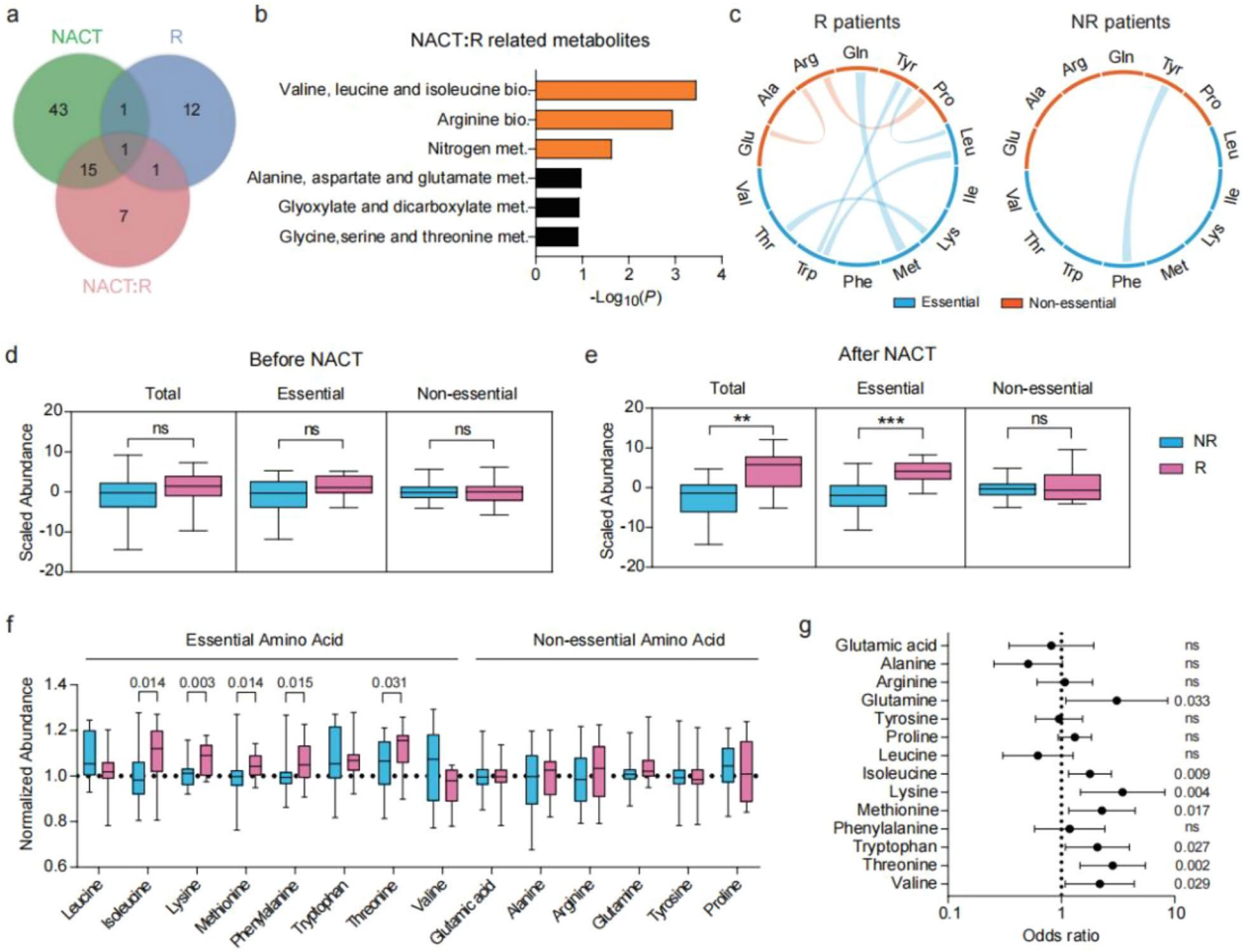

Fig. 5 Achieving R to NACT may be attributed to elevated essential amino acids. **a** Differentially changed metabolites associated with NACT treatment and R status, and the combination of both using a two-way ANOVA analysis ($P < 0.05$). **b** Pathway enrichment analysis of metabolites related to both NACT treatment and R status (Hypergeometric test; $P < 0.05$). **c** Metabolic correlation between two amino acids in R and NR patients (Pearson correlation; $r > 0.50$ and two-sided Student's t test $P < 0.05$). **d, e** Amino acid levels in serum samples from R (n = 18) and NR (n = 32) patients before and after NACT treatment: **c**, before NACT at baseline; **d**, after NACT (Two-sided Wilcoxon test; ns, not significant; ***, $P < 0.001$; **, $P < 0.01$). **f** Amino acid levels in serum samples from R (n = 18) and NR (n = 32) patients after NACT treatment. Data normalized to baseline levels (Two-sided Wilcoxon test). **g** Odd ratios of amino acids related to R status after NACT (two-sided z-test of logistic regression; ns, not significant). R (n = 18) and NR (n = 32). Error bars represent 95% confidence intervals

with LABC to NACT treatment and R status. In particular, baseline levels of essential amino acids did not differ before NACT, but after NACT, patient serum samples significantly increased in these amino acids. These data also suggest that dietary and nutritional interventions, especially supplementation with essential amino acids during NACT, may positively contribute to tumor regression in patients with LABC.

Discussion

This study characterized the serum metabolic profile of patients with LABC receiving NACT and identified reactive metabolic features associated with the treatment process and therapeutic response. Our preliminary analysis revealed significant differences in metabolic reactions before and after NACT. Amino acid metabolism pathways, including phenylalanine, tyrosine, and tryptophan biosynthesis; arginine biosynthesis; and valine, leucine, and isoleucine biosynthesis, were substantially impacted by NACT treatment. We discovered that following NACT treatment, metabolites of tryptophan metabolism, including tryptophan, indole-3-propionic acid, and indole-3-lactic acid, decreased (Additional file 6: Fig. S5). Wang et al. suggested that irinotecan-induced intestinal injury in mice led to the upregulation of tryptophan metabolism [37]. However, Ahmed et al. reported that

elevated tryptophan metabolite levels in tumor cells enhance tumor malignancy through aryl hydrocarbon receptor activation [38]. In our cohort of patients with LABC, the reduction in tryptophan metabolites discovered indicates a more significant role for the latter. Moreover, the sphingolipid metabolism pathway significantly impacted the response to NACT. We found that the metabolites of sphingolipid metabolism, such as sphingosine, sphingosine-1-phosphate (S1P), and ethanolamine phosphate, were exclusively reduced after NACT (Additional file 6: Fig. S6a). Previous clinical trials and mouse model studies on head and neck cancer have confirmed a significant alteration in the serum levels of C18 ceramide associated with doxorubicin-related chemotherapy drug treatment [39, 40]. Furthermore, the abnormal upregulation of sphingolipid metabolism leading to the generation of glycosylated ceramide and/or S1P resulted in drug resistance to chemotherapy in breast cancer and other tumors [41–43]. Consequently, we compared the levels of sphingolipid metabolites in the serum of R and NR patients before and after treatment. While their levels decreased after NACT treatment, the levels of sphingosine and S1P in NR patients were significantly higher than those in R patients post-NACT treatment (Additional file 6: Fig. S6b). Conversely, S1P can promote cancer growth and metastasis through S1PR-dependent or S1PR-independent signaling pathways [44, 45]. Given its function in controlling tumor development and mediating chemotherapy efficacy, the reduction in sphingolipid metabolites found in the serum of patients after NACT treatment and the higher levels of sphingolipid metabolites in NR patients than in R patients may be explicable.

Chemotherapy often accompanies hematological adverse events, including anemia, leukopenia, thrombocytopenia, and neutropenia, which reduce the efficacy of NACT treatment. Current studies on the relationship between serum metabolites and hematological adverse events are relatively limited. We successfully established the relationship between baseline metabolite levels and common hematologic toxicities, such as Hb, WBC, PLT, and NEUT values. We observed that metabolites associated with WBC and NEUT were enriched in the phenylalanine, tyrosine, and tryptophan biosynthesis and D-amino acid metabolism pathways, while those linked to Hb and PLT were enriched in pyrimidine metabolism. These results demonstrated the potential of pre-treatment serum metabolomic profiles to identify individuals at high risk of NACT-induced hematological toxicity, potentially enabling personalized treatment for patients with LABC.

An interesting discovery of this study is the subtype differences in carnitine metabolism associated with the R status after NACT. Notably, an increasing number of clinical trials have shown that breast cancer subtypes significantly contribute to variability in R status following NACT, with patients with non-luminal subtypes consistently exhibiting lower response rates [6, 7]. We observed that among all R patients, the serum carnitine levels in patients with non-luminal breast cancer were significantly lower than those in patients with luminal breast cancer. Acylcarnitines are crucial metabolic intermediates in the β-oxidation of fatty acids, serving as a pivotal energy source for cellular growth and proliferation [46]. Estrogens reduce β-oxidation by targeting carnitine palmitoyltransferase [47, 48], yet the expression of estrogen receptors in patients with luminal breast cancer may competitively counteract this effect. Current research has reported that carnitine possesses the efficacy to mitigate multi-organ toxicity and systemic fatigue induced by chemotherapy [49, 50]. The interrelationship between carnitine metabolism mediated by breast cancer subtypes and the R status in response to NACT remains unclear. Our findings suggest that in NACT, carnitine supplementation in patients with LABC should be vigilant, which may lead to reduced sensitivity to chemotherapy. However, more clinical and experimental studies are necessary.

After NACT treatment, only 20%–30% of patients with LABC achieved a complete pathologic response [6, 7]. As the state of complete pathological response cannot be confirmed before surgery, a pre-surgery examination for R status prediction is valuable for selecting follow-up treatment. We observed that the levels of hypoxanthine and PC (36:3) were significantly higher in R patients than in NR patients, while leucine levels were lower. And we successfully developed a robust predictive model for NACT efficacy using these three metabolites in combination with another clinical marker, molecular subtype. Hypoxanthine is a purine and an intermediate in the metabolism of adenosine, as well as in nucleic acid synthesis via the salvage pathway. Hypoxanthine has long been established as a biomarker of hypoxia [51]. Shakartalla et al. identified that hypoxanthine as a novel metastasis-associated metabolite in breast cancer [52] and another study demonstrated that plasma hypoxanthine could serve as a potential biomarker for the diagnosis of breast cancer [53]. PC (36:3) is a phosphatidylcholine in which the acyl groups at positions C-1 and C-2 contain a total of 36 carbon atoms and 3 double bonds. To date, no studies have explored the involvement of PC (36:3) in tumorigenesis and treatment. However, studies have shown that the metabolism of phosphatidylcholine generates lipid mediators that can modulate immune cell function, thereby influencing the growth, survival, proliferation, and treatment resistance of cancer cells [54]. Leucine, together with isoleucine and valine, constitutes

the three essential branched-chain amino acids (BCAAs), which play a critical role in cellular metabolism and protein synthesis. Studies have demonstrated that BCAA metabolism was significantly upregulated in breast cancer, with BCAT1-mediated activation of mTOR driving mitochondrial biogenesis and enhancing mitochondrial function, and subsequently promotes the growth and colony formation of breast cancer cells [55]. However, some studies have reported that elevated levels of BCAAs can inhibit tumor growth and metastasis in breast cancer, suggesting that increasing dietary BCAA intake may offer potential therapeutic benefits in the management of the disease [56, 57]. Consequently, BCAAs play a dual role in cancer, with their effects on tumor growth or suppression being highly dependent on specific conditions and concentrations [58].

As far as leucine alone, it has a controversial role in hepatocellular carcinoma, whereas its predominantly pro-tumor effect in breast cancer has been demonstrated in multiple studies [59]. By activating mTORC1, leucine drives metabolic reprogramming that promotes glycolysis and anabolism, processes associated with enhanced tumorigenesis and treatment resistance [60]. Xiao et al. demonstrated that leucine deprivation inhibits proliferation and induces apoptosis in human breast cancer cells through the modulation of fatty acid synthase [61]. Recent studies have also shown that elevated plasma leucine levels induced by the microbiota were associated with increased tumor infiltration by polymorphonucler myeloid-derived suppressor cells and adverse clinical outcomes in patients with breast cancer [62]. Additionally, Yasuhiro et al. showed that a diet high in leucine may promote drug resistance in breast cancer [63]. Therefore, we speculated that leucine may influence the NACT treatment response. However, in our findings, a higher content of essential amino acids (including isoleucine, lysine, methionine, tryptophan, threonine, and valine) in the serum of patients with LABC after NACT treatment was positively correlated with the therapeutic response. Essential amino acids and their metabolites are important in tumor biology and treatment [64]. Presently, many studies have reported that supplementation of essential amino acids enhances the efficacy of tumor treatment [65, 66]. These findings suggest that nutritional interventions supplemented with essential amino acids may improve the responsiveness of NR patients to NACT. However, further clinical trials are warranted to validate this intervention before its implementation in clinical practice.

The potential use of omics analysis in NACT for breast cancer and other cancers has been shown in earlier studies [18, 25, 67–70]. For example, Diaz et al. identified that patients with triple-negative breast cancer can be categorized using glycohyocholic and glycodeoxycholic acids based on their response to NACT treatment [25]. Rebecca et al. showed that mesenchymal subtype ovarian cancer tissues exhibited distinct metabolomics profiles compared with other subtypes, and their ascites demonstrate significant alterations in immune responses and signaling pathways [69]. Feng et al. performed metabolomics analysis in patients undergoing NACT for prostate cancer and identified the downregulation of key pathways in biosynthesis and energy metabolism, thereby inhibiting tumor growth [70]. However, longitudinal analysis of the process before and after NACT treatment is rare in study design. Compared with previous studies, this research differs in design and technology in the following aspects: (1) The pre- and post-treatment analyses conducted in this longitudinal investigation can yield important information about the dynamic metabolic profile of the NACT response in patients with LABC. (2) Postoperative pathological MP grading served as the clinical determination in this study, offering a more stringent and meticulous clinical assessment.

However, this study has some limitations. This study aimed to identify prospective metabolites that may be connected to the NACT treatment process and therapeutic response, rather than construct a clinical trial to anticipate the reaction to NACT, which would require the absolute concentrations of metabolites. Consequently, our study opted for a non-targeted detection approach rather than a targeted quantitative measurement method to compare the correlation between metabolites and NACT treatment. The study's small sample size and the absence of detection points during treatment are potential limitations that require further analysis in larger cohorts. In addition, our methodology solely employed RPLC without the concurrent use of hydrophilic interaction liquid chromatography for detection, which may have resulted in incomplete coverage of the metabolites being identified. Furthermore, it is evident that this study's pathway enrichment analysis, which was based on differential metabolites in the circulation metabolome rather than the tissue or cellular metabolome, is inadequate for determining the metabolic pathways that NACT treatment first altered. However, obtaining tissue samples directly from patient multiple times is highly challenging. In summary, we report a model based on serum non-target metabolomics signatures for predicting responses and toxicities of NACT treatment. Furthermore, our primary findings demonstrated the characteristic metabolite changes before and after NACT treatment and provided potential benefits for the treatment of patients with LABC in clinical practice.

Supplementary Information

The online version contains supplementary material available at https://doi.org/10.1186/s13058-024-01956-w.

Additional file 1. Metabolite annotation and quantification results of the whole dataset.

Additional file 2. The 60 significantly changed metabolites associated with the NACT treatment.

Additional file 3. The 53 metabolites associated with the hematological toxicities of NACT treatment.

Additional file 4. Levels of acylcarnitines used for data analysis.

Additional file 5. Levels of amino acids between R and NR patients used for data analysis.

Additional file 6. Supplementary material for "Serum Metabolomic Profiling for Predicting Therapeutic Response and Toxicity in Breast Cancer Neoadjuvant Chemotherapy: A Retrospective Longitudinal Study".

Acknowledgements
We would like to extend our gratitude to Home for Researchers editorial team (www.home-for-researchers.com) for language editing service.

Author contributions
F.Z., G.C., and H.J. designed the study. F.Z., X.Q., and C.Y. collected the specimens. F.Z. and S.X. performed LC–MS/MS detection. F.Z., R.G., and K.S. conducted data analysis. F.Z., R.G., and K.S. wrote the manuscript. All authors reviewed the manuscript.

Funding
The National Key R&D Program of China (2022YFA1105200), Joint Funds of the National Natural Science Foundation of China (U22A20321), Key Program of National Natural Science Foundation of China (81930079), and Key R&D Program of Zhejiang Province (2022C03019) were used.

Availiability of data materials
No datasets were generated or analysed during the current study.

Declarations

Ethics approval and consent to participate
The serum of LABC patients was obtained from the Department of Clinical Laboratory, SAHZU. All patients provided written informed consent prior to the study. The Institutional Research Ethics Committee approved the use of clinical specimens for research purposes.

Consent for publication
Not applicable.

Competing of interests
The authors declare no competing interests.

Author details
[1]Department of Breast Surgery, Second Affiliated Hospital, Zhejiang University School of Medicine, Jiefang Road, Hangzhou, Zhejiang, China. [2]Key Laboratory of Tumor Microenvironment and Immune Therapy of Zhejiang Province, Second Affiliated Hospital, Zhejiang University School of Medicine, Hangzhou, Zhejiang, China. [3]Cancer Institute (Key Laboratory of Cancer Prevention and Intervention, China National Ministry of Education), Second Affiliated Hospital, Zhejiang University School of Medicine, Hangzhou, Zhejiang, China. [4]Cancer Center, Zhejiang University, Hangzhou, Zhejiang, China. [5]Department of Laboratory Medicine, The Second Affiliated Hospital of Zhejiang University School of Medicine, Hangzhou, Zhejiang, China. [6]Analytical Instrument Trading Co., Ltd, SCIEX, Shanghai, China.

Received: 6 November 2024 Accepted: 20 December 2024
Published online: 06 January 2025

References

1. Sedeta ET, Jobre B, Avezbakiyev B. Breast cancer: Global patterns of incidence, mortality, and trends. 2023; 41(16_suppl):10528
2. Trabulsi NH, Shabkah AA, Ujaimi R, Iskanderani O, Kadi MS, Aljabri N, et al. Locally advanced breast cancer: treatment patterns and predictors of survival in a saudi tertiary center. Cureus. 2021;13(6):e15526.
3. Dhanushkodi M, Sridevi V, Shanta V, Rama R, Swaminathan R, Selvaluxmy G, et al. Locally advanced breast cancer (LABC): real-world outcome of patients from cancer institute. Chennai JCO Glob Oncol. 2021;7:767–81.
4. Aebi S, Karlsson P, Wapnir IL. Locally advanced breast cancer. Breast (Edinburgh, Scotland). 2022;62 Suppl 1(Suppl 1):S58-s62.
5. Costa R, Hansen N, Gradishar WJ. 63 - Locally Advanced Breast Cancer. In: Bland KI, Copeland EM, Klimberg VS, Gradishar WJ, editors. The Breast (Fifth Edition): Elsevier; 2018. p. 819–31.e6.
6. Antonini M, Mattar A, Bauk Richter FG, Pannain GD, Teixeira MD, Amorim AG, et al. Real-world evidence of neoadjuvant chemotherapy for breast cancer treatment in a Brazilian multicenter cohort: correlation of pathological complete response with overall survival. The Breast. 2023;72:103577.
7. Choudhary P, Gogia A, Deo S, Mathur S, Sharma D. Neoadjuvant chemotherapy in locally advanced breast cancer: Clinicopathological characteristics and correlation with pathological complete response. 2020;38(15_suppl):e12658-e.
8. Conti M, Morciano F, Bufi E, D'Angelo A, Panico C, Di Paola V, et al. Surgical planning after neoadjuvant treatment in breast cancer: a multimodality imaging-based approach focused on MRI. Cancers. 2023;15(5):96.
9. Reinisch M, von Minckwitz G, Harbeck N, Janni W, Kümmel S, Kaufmann M, et al. Side effects of standard adjuvant and neoadjuvant chemotherapy regimens according to age groups in primary breast cancer. Breast Care (Basel, Switzerland). 2013;8(1):60–6.
10. Tan AR, Im SA, Mattar A, Colomer R, Stroyakovskii D, Nowecki Z, et al. Fixed-dose combination of pertuzumab and trastuzumab for subcutaneous injection plus chemotherapy in HER2-positive early breast cancer (FeDeriCa): a randomised, open-label, multicentre, non-inferiority, phase 3 study. Lancet Oncol. 2021;22(1):85–97.
11. Antolin S, García-Caballero L, Reboredo C, Diaz AM, Mosquera J, Vázquez-Boquete A, et al. Correlation between HER2 amplification level and response to neoadjuvant treatment with trastuzumab and chemotherapy in HER2 positive breast cancer. 2020;38(15_suppl):e12641-e.
12. Bilici A, Olmez OF, Sezer A, Oksuzoglu B, Kaplan MA, Karadurmus N, et al. Real-life analysis of pathologic complete response with neoadjuvant trastuzumab plus taxane with or without pertuzumab therapy in HER2 positive locally-advanced breast cancer (HER2PATH Study). 2022;40(16_suppl):e12610-e.
13. Wang X, Hao X, Yan J, Xu J, Hu D, Ji F, et al. Urine biomarkers discovery by metabolomics and machine learning for Parkinson's disease diagnoses. Chin Chem Lett. 2023;34(10):108230.
14. Gu Y-H, Chen Y, Li Q, Xie N-B, Xing X, Xiong J, et al. Metabolome profiling by widely-targeted metabolomics and biomarker panel selection using machine-learning for patients in different stages of chronic kidney disease. Chin Chem Lett. 2024;35(11):109627.
15. Tan J, Le A. The heterogeneity of breast cancer metabolism. Adv Exp Med Biol. 2021;1311:89–101.
16. Coronel-Hernández J, Pérez-Yépez EA, Delgado-Waldo I, Contreras-Romero C, Jacobo-Herrera N, Cantú-De León D, et al. Aberrant metabolism as inductor of epigenetic changes in breast cancer: therapeutic opportunities. Front Oncol. 2021;11:676562.
17. Zheng X, Ma H, Wang J, Huang M, Fu D, Qin L, et al. Energy metabolism pathways in breast cancer progression: the reprogramming, crosstalk, and potential therapeutic targets. Transl Oncol. 2022;26:101534.
18. Lyon DE, Yao Y, Garrett T, Kelly DL, Cousin L, Archer KJ. Comparison of serum metabolomics in women with breast Cancer Prior to Chemotherapy and at 1 year: cardiometabolic implications. BMC Womens Health. 2023;23(1):221.
19. Peterson AL, Walker AK, Sloan EK, Creek DJ. Optimized method for untargeted metabolomics analysis of MDA-MB-231 breast cancer. Cells. 2016;6(4):30.
20. Maria RM, Altei WF, Selistre-de-Araujo HS, Colnago LA. Impact of chemotherapy on metabolic reprogramming: characterization of the metabolic profile of breast cancer MDA-MB-231 cells using 1H HR-MAS NMR spectroscopy. J Pharm Biomed Anal. 2017;146:324–8.

21. Cardoso MR, Santos JC, Ribeiro ML, Talarico MCR, Viana LR, Derchain SFM. A metabolomic approach to predict breast cancer behavior and chemotherapy response. Int J Mol Sci. 2018;19(2):963.
22. Cardoso MR, Silva AAR, Talarico MCR, Sanches PHG, Sforça ML, Rocco SA, et al. Metabolomics by NMR combined with machine learning to predict neoadjuvant chemotherapy response for breast cancer. Cancers. 2022;14(20):62.
23. Ogston KN, Miller ID, Payne S, Hutcheon AW, Sarkar TK, Smith I, et al. A new histological grading system to assess response of breast cancers to primary chemotherapy: prognostic significance and survival. Breast (Edinburgh, Scotland). 2003;12(5):320–7.
24. Zhu Q, Ademuyiwa FO, Young C, Appleton C, Covington MF, Ma C, et al. Early assessment window for predicting breast cancer neoadjuvant therapy using biomarkers, ultrasound, and diffuse optical tomography. Breast Cancer Res Treat. 2021;188(3):615–30.
25. Díaz C, González-Olmedo C, Díaz-Beltrán L, Camacho J, Mena García P, Martín-Blázquez A, et al. Predicting dynamic response to neoadjuvant chemotherapy in breast cancer: a novel metabolomics approach. Mol Oncol. 2022;16(14):2658–71.
26. Benton HP, Ivanisevic J, Mahieu NG, Kurczy ME, Johnson CH, Franco L, et al. Autonomous metabolomics for rapid metabolite identification in global profiling. Anal Chem. 2015;87(2):884–91.
27. Shen X, Wang R, Xiong X, Yin Y, Cai Y, Ma Z, et al. Metabolic reaction network-based recursive metabolite annotation for untargeted metabolomics. Nat Commun. 2019;10(1):1516.
28. Zhou Z, Luo M, Zhang H, Yin Y, Cai Y, Zhu ZJ. Metabolite annotation from knowns to unknowns through knowledge-guided multi-layer metabolic networking. Nat Commun. 2022;13(1):6656.
29. Chambers MC, Maclean B, Burke R, Amodei D, Ruderman DL, Neumann S, et al. A cross-platform toolkit for mass spectrometry and proteomics. Nat Biotechnol. 2012;30(10):918–20.
30. Tsugawa H, Cajka T, Kind T, Ma Y, Higgins B, Ikeda K, et al. MS-DIAL: data-independent MS/MS deconvolution for comprehensive metabolome analysis. Nat Methods. 2015;12(6):523–6.
31. Altman NS. An introduction to Kernel and nearest-neighbor nonparametric regression. Am Stat. 1992;46(3):175–85.
32. Fiehn O, Robertson D, Griffin J, van der Werf M, Nikolau B, Morrison N, et al. The metabolomics standards initiative (MSI). Metabolomics. 2007;3(3):175–8.
33. R Core Team R. R: A language and environment for statistical computing. 2013.
34. Pang Z, Chong J, Zhou G, de Lima Morais DA, Chang L, Barrette M, et al. MetaboAnalyst 5.0: narrowing the gap between raw spectra and functional insights. Nucleic Acids Res. 2021;49(W1):W388–96.
35. Kanehisa M, Goto S, Sato Y, Kawashima M, Furumichi M, Tanabe M. Data, information, knowledge and principle: back to metabolism in KEGG. Nucleic Acids Res. 2014;42:D199-205.
36. Zou HJJotASA. The adaptive lasso and its oracle properties. 2006;101:1418 - 29.
37. Wang D, Li D, Zhang Y, Chen J, Zhang Y, Liao C, et al. Functional metabolomics reveal the role of AHR/GPR35 mediated kynurenic acid gradient sensing in chemotherapy-induced intestinal damage. Acta Pharm Sinica B. 2021;11(3):763–80.
38. Sadik A, Somarribas Patterson LF, Öztürk S, Mohapatra SR, Panitz V, Secker PF, et al. IL4I1 Is a metabolic immune checkpoint that activates the AHR and promotes tumor progression. Cell. 2020;182(5):1252-70.e34.
39. Saddoughi SA, Garrett-Mayer E, Chaudhary U, O'Brien PE, Afrin LB, Day TA, et al. Results of a phase II trial of gemcitabine plus doxorubicin in patients with recurrent head and neck cancers: serum C_{18}-ceramide as a novel biomarker for monitoring response. Clini Cancer Res. 2011;17(18):6097–105.
40. Senkal CE, Ponnusamy S, Rossi MJ, Bialewski J, Sinha D, Jiang JC, et al. Role of human longevity assurance gene 1 and C18-ceramide in chemotherapy-induced cell death in human head and neck squamous cell carcinomas. Mol Cancer Ther. 2007;6(2):712–22.
41. Zhang X, Wu X, Su P, Gao Y, Meng B, Sun Y, et al. Doxorubicin influences the expression of glucosylceramide synthase in invasive ductal breast cancer. PLoS ONE. 2012;7(11):e48492.
42. Huang X, Taeb S, Jahangiri S, Emmenegger U, Tran E, Bruce J, et al. miRNA-95 mediates radioresistance in tumors by targeting the sphingolipid phosphatase SGPP1. Can Res. 2013;73(23):6972–86.
43. Ogretmen B. Sphingolipid metabolism in cancer signalling and therapy. Nat Rev Cancer. 2018;18(1):33–50.
44. Pitson SM, Moretti PA, Zebol JR, Lynn HE, Xia P, Vadas MA, et al. Activation of sphingosine kinase 1 by ERK1/2-mediated phosphorylation. EMBO J. 2003;22(20):5491–500.
45. Takabe K, Kim RH, Allegood JC, Mitra P, Ramachandran S, Nagahashi M, et al. Estradiol induces export of sphingosine 1-phosphate from breast cancer cells via ABCC1 and ABCG2. J Biol Chem. 2010;285(14):10477–86.
46. Qu Q, Zeng F, Liu X, Wang QJ, Deng F. Fatty acid oxidation and carnitine palmitoyltransferase I: emerging therapeutic targets in cancer. Cell Death Dis. 2016;7(5):e2226.
47. Linher-Melville K, Zantinge S, Sanli T, Gerstein H, Tsakiridis T, Singh G. Establishing a relationship between prolactin and altered fatty acid β-oxidation via carnitine palmitoyl transferase 1 in breast cancer cells. BMC Cancer. 2011;11:56.
48. Juraszek B, Nałęcz KA. SLC22A5 (OCTN2) carnitine transporter-indispensable for cell metabolism, a Jekyll and hyde of human cancer. Molecules (Basel, Switzerland). 2019;25(1):69.
49. Matsui H, Einama T, Shichi S, Kanazawa R, Shibuya K, Suzuki T, et al. L-Carnitine supplementation reduces the general fatigue of cancer patients during chemotherapy. Mol Clin Oncol. 2018;8(3):413–6.
50. Sayed-Ahmed MM. Role of carnitine in cancer chemotherapy-induced multiple organ toxicity. Saudi Pharm J. 2010;18(4):195–206.
51. Saugstad OD. Hypoxanthine as a measurement of hypoxia. Pediatr Res. 1975;9(4):158–61.
52. Shakartalla SB, Ashmawy NS, Semreen MH, Fayed B, Al Shareef ZM, Jayakumar MN, et al. (1)H-NMR metabolomics analysis identifies hypoxanthine as a novel metastasis-associated metabolite in breast cancer. Sci Rep. 2024;14(1):253.
53. Park J, Shin Y, Kim TH, Kim DH, Lee A. Plasma metabolites as possible biomarkers for diagnosis of breast cancer. PLoS ONE. 2019;14(12):e0225129.
54. Saito RF, Andrade LNS, Bustos SO, Chammas R. Phosphatidylcholine-derived lipid mediators: the crosstalk between cancer cells and immune cells. Front Immunol. 2022;13:768606.
55. Zhang L, Han J. Branched-chain amino acid transaminase 1 (BCAT1) promotes the growth of breast cancer cells through improving mTOR-mediated mitochondrial biogenesis and function. Biochem Biophys Res Commun. 2017;486(2):224–31.
56. Chi R, Yao C, Chen S, Liu Y, He Y, Zhang J, et al. Elevated BCAA suppresses the development and metastasis of breast cancer. Front Oncol. 2022;12:887257.
57. Nouri-Majd S, Salari-Moghaddam A, Benisi-Kohansal S, Azadbakht L, Esmaillzadeh A. Dietary intake of branched-chain amino acids in relation to the risk of breast cancer. Breast Cancer (Tokyo, Japan). 2022;29(6):993–1000.
58. Xu E, Ji B, Jin K, Chen Y. Branched-chain amino acids catabolism and cancer progression: focus on therapeutic interventions. Front Oncol. 2023;13:1220638.
59. Akbay B, Omarova Z, Trofimov A, Sailike B, Karapina O, Molnár F, et al. Double-edge effects of leucine on cancer cells. Biomolecules. 2024;14(11):96.
60. Wolfson RL, Chantranupong L, Saxton RA, Shen K, Scaria SM, Cantor JR, et al. Sestrin2 is a leucine sensor for the mTORC1 pathway. Science. 2016;351(6268):43–8.
61. Xiao F, Wang C, Yin H, Yu J, Chen S, Fang J, et al. Leucine deprivation inhibits proliferation and induces apoptosis of human breast cancer cells via fatty acid synthase. Oncotarget. 2016;7(39):63679–89.
62. Chen J, Liu X, Zou Y, Gong J, Ge Z, Lin X, et al. A high-fat diet promotes cancer progression by inducing gut microbiota-mediated leucine production and PMN-MDSC differentiation. Proc Natl Acad Sci USA. 2024;121(20):e2306776121.
63. Saito Y, Li L, Coyaud E, Luna A, Sander C, Raught B, et al. LLGL2 rescues nutrient stress by promoting leucine uptake in ER(+) breast cancer. Nature. 2019;569(7755):275–9.
64. Chen J, Cui L, Lu S, Xu S. Amino acid metabolism in tumor biology and therapy. Cell Death Dis. 2024;15(1):42.
65. Bonfili L, Cecarini V, Cuccioloni M, Angeletti M, Flati V, Corsetti G, et al. Essential amino acid mixtures drive cancer cells to apoptosis through proteasome inhibition and autophagy activation. FEBS J. 2017;284(11):1726–37.

66. Wang H, Jia H, Gao Y, Zhang H, Fan J, Zhang L, et al. Serum metabolic traits reveal therapeutic toxicities and responses of neoadjuvant chemoradiotherapy in patients with rectal cancer. Nat Commun. 2022;13(1):7802.
67. Wei S, Liu L, Zhang J, Bowers J, Gowda GA, Seeger H, et al. Metabolomics approach for predicting response to neoadjuvant chemotherapy for breast cancer. Mol Oncol. 2013;7(3):297–307.
68. Wang J, Yu P, Luo J, Sun Z, Yu J, Wang J. Transcriptomic and microRNA expression profiles identify biomarkers for predicting neo-chemoradiotherapy response in esophageal squamous cell carcinomas (ESCC). Front Pharmacol. 2021;12:626972.
69. Arend RC, Scalise CB, Gordon ER, Davis AM, Foxall ME, Johnston BE, et al. Metabolic alterations and WNT signaling impact immune response in HGSOC. Clini Cancer Res. 2022;28(7):1433–45.
70. Qu F, Gu Y, Xue M, He M, Zhou F, Wang G, et al. Impact of therapy on cancer metabolism in high-risk localized prostate cancer treated with neoadjuvant docetaxel and androgen deprivation therapy. Prostate. 2021;81(9):560–71.

Publisher's Note